PHYSICAL REVIEW B VOLUME 51, NUMBER 23 15 JUNE 1995-I

Magnetothermopower oscillations in a lateral superlattice

R. Taboryski,* B. Brosh, M. Y. Simmons, D. A. Ritchie, C. J. B. Ford, and M. Pepper
Cavendish Laboratory, Madingley Road, Cambridge CB3 0HE, United Kingdom
(Received 27 January 1995)

We present a measurement of the magnetothermopower oscillations in a weak lateral superlattice potential imposed on a high-mobility two-dimensional electron gas (2DEG). Our samples showed clear commensurability as well as Shubnikov–de Haas oscillations in both the longitudinal resistance and the thermopower as a function of magnetic field applied perpendicular to the 2DEG. We used a local electron-heating technique to generate a temperature gradient across the superlattice. We find good agreement with existing theory.

In 1988 Weiss *et al.*[1] reported a type of magnetoresistance periodic in $1/B$, imposed by a weak modulation of the two-dimensional carrier density in a GaAs/$Al_xGa_{1-x}As$ heterostructure. The modulation was induced by a holographic illumination of the sample with a separation of the interference fringes of 382 nm. Other techniques for making the superlattices were, however, soon developed.[2,3] The observed magnetoresistance oscillations were subsequently explained in terms of a commensurability relation

$$2R_c=(n+1/4)a, \tag{1}$$

between the superlattice period a and the cyclotron radius $R_c=m v_F/eB_n$ of the electron,[2,4,5] where B_n are the magnetic fields corresponding to maxima in the longitudinal resistance. In the literature the magnetoresistance oscillations have thus been referred to as either commensurability oscillations or Weiss oscillations, after their discoverer. Theoretically the oscillations in $\rho_{xx}(B)$ (i.e., current flow perpendicular to the stripes) are well understood in a semiclassical picture proposed by Beenakker[5] as guiding center drift resonances of the cyclotron orbits, or in a quantum-mechanical approach as a modulation of the Landau bandwidth,[2,4,6–8] which also explains the much weaker oscillations observed in $\rho_{yy}(B)$. The oscillations in ρ_{yy} are found both experimentally and theoretically to be 180° out of phase relative to the dominating oscillations in ρ_{xx}. Despite this early insight, the effect has caused a continuous interest in recent years.[9–11]

In this paper we present measurements of the diffusion thermopower $S_{xx}(B)=\Delta V_x(B)/\Delta T_x$ of a high mobility two-dimensional electron gas (2DEG) with a one-dimensional lateral modulation. Theoretically it has been predicted that the oscillations in the thermopower should be dominated by the collisional contribution to the conductivity.[13] This contribution, which is also responsible for the more subtle oscillations in ρ_{yy}, has been calculated in a quantum-mechanical approach using a hopping-type Kubo formula for transport in the presence of a magnetic field. The theory predicts that $S_{xx}\approx S_{yy}$, and that the oscillations in the thermopower should be 90° out of phase relative to the oscillations in ρ_{xx}.

In our experiment, the lateral modulation was imposed by a surface NiCr/Au grating gate with a period of 400 nm, shown as $g2$ in the inset of Fig. 3. The amplitude of the modulation could be controlled by a gate voltage applied to the grating. However, the most clear magnetoresistance oscillations were observed with the gate grounded, and the data presented in this paper are thus obtained with $g2$ grounded. In this case the potential modulation is induced in the piezoelectric GaAs by elastic strain caused by different thermal expansion coefficients in GaAs and the gate material[10] as the device is cooled down. The GaAs/$Al_xGa_{1-x}As$ heterostructure we used for our measurements had the 2DEG embedded approximately 100 nm under the surface. Samples were illuminated with a red-light-emitting diode at temperatures below 6 K before measurements commenced. Ungated samples made from the same heterostructure had a carrier density of 3.5×10^{15} m^{-2} and a mobility of 180 m^2/V s under full illumination conditions. Gated samples usually had a somewhat smaller carrier density, between 2.8 and 3.2×10^{15} m^{-2}. The

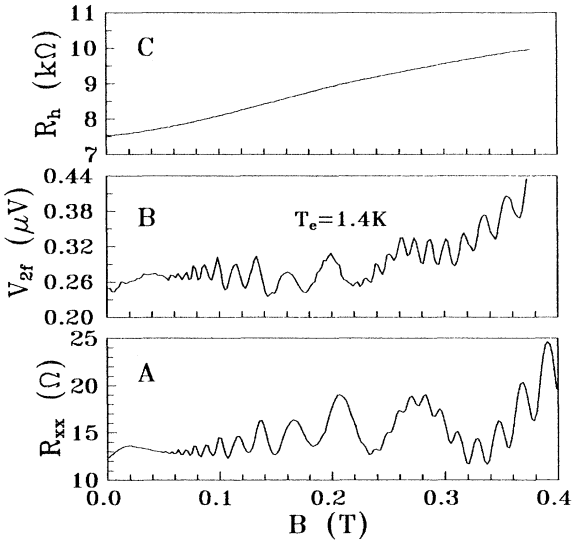

FIG. 1. Magnetoresistance (A) and second-harmonic thermopower voltage (B). The two curves were obtained from the same sample; however, the magnetic-field axis for the two curves has been corrected for a small difference in carrier density that occurred between the two measurements. The heating current used in the $2f$ measurement was 1.2 μA. The peculiar peak amplitude variation is an artifact of this particular sample, but makes it easy to identify each peak in the $2f$ signal. (C) The heating resistance measured simultaneously with the V_{2f} curve shown in the lower panel. The heating resistance was measured in a two-probe configuration with a gate voltage $V_{g1}=-0.1$ V.

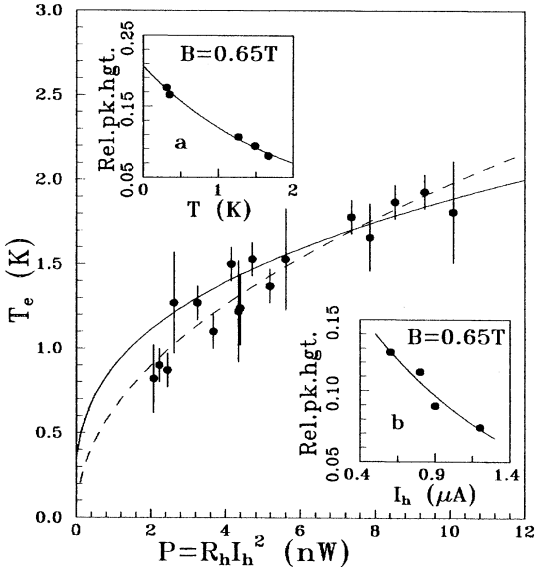

FIG. 2. Electron temperature in the region under the heating gate vs dissipated power in the heating resistance. The solid curve is a best fit to Eq. (2), while the dashed curve is the best empirical power-law fit. Inset (a) shows an example of a SdH relative-peak-height dependence on temperature for a peak in the heating resistance at $B=0.65$ T. The solid line is a exponential fit to the data points. Inset (b) shows the peak-height dependence on heating current for the same SdH peak.

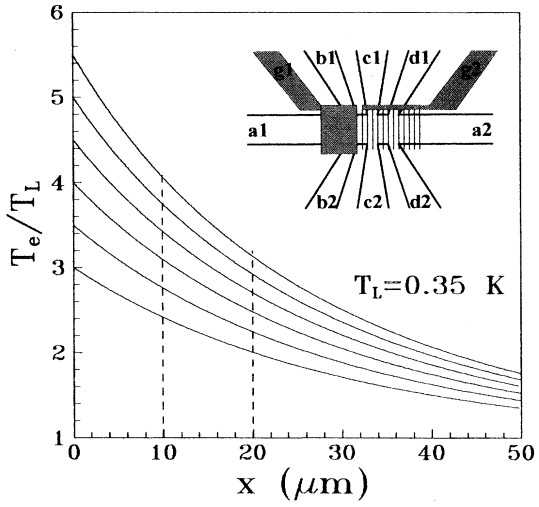

FIG. 3. Calculated electron-temperature-decay profiles along the Hall bar depicted in the inset for various boundary conditions at $x=0$, i.e., between probes $b1$ and $b2$. The curves have been calculated by Eq. (4) with $\gamma=3$. The lattice temperature used in the calculation was 0.35 K, the same as the bath temperature in the experiment. The vertical dashed lines at 10 and 20 μm mark the distance to the voltage probes $(c1,c2)$ and $(d1,d2)$ respectively. The probes $a1$ and $a2$ were used as current probes in a conventional measurement of the longitudinal resistance R_{xx}. The gate $g2$ was connected on the grating on the Hall bar, but grounded in our experiments.

magnetoresistance $\rho_{xx}(B)$ was measured using a standard phase-sensitive current-controlled measuring scheme with the current passed between contacts $a1$ and $a2$, and the voltage measured across either $c1$ and $d1$ or across $c2$ and $d2$ (the contact denominations refer to the inset of Fig. 3). The width of the etched Hall bar in our devices was 20 μm, while the distance between two consecutive pairs of probes (b,c,d) was chosen to be approximately 10 μm, which is shorter than the mean free path l in the 2DEG. For the ungated devices, $l=17.5$ μm. The lower trace shown in Fig. 1 is the measured magnetoresistance. The last maxima shown, corresponding to $n=2$ in Eq. (1), occurs at about 0.28 T in the figure. For the best of our samples, peaks up to $n=19$ were detected. The fast oscillations superimposed on the commensurability oscillations in the high-field end of the curve are Shubnikov–de Haas oscillations. The reason why the $n=1$ peak is not shown will be explained shortly. The thermopower measurements were done with the so-called local-heating technique, where the temperature gradient was induced by locally heating up the electron gas by a high current. This technique works because the dissipated power is quickly distributed among the electrons via the fast electron-electron interaction rate before it is lost to the lattice via the slower electron-phonon interactions. The electron temperature will stabilize at a level were the dissipated power equals the heat loss to the phonons. The advantage of the technique is that only the temperature of the electron gas is elevated while the lattice temperature remains unchanged.[14] This technique has been successfully used to investigate the properties of other transport phenomena.[15] The upper trace in the lower panel of Fig. 1 is the measured thermopower voltage $(=S_{xx}\Delta T)$. This voltage was obtained by passing an ac heating current I_h between the contacts $b1$ and $b2$, and measuring the thermopower voltage as the second-harmonic differential voltage response across contacts $c1$ and $d1$ (or $c2$ and $d2$). The short distance between the probe pairs was chosen for the imposed temperature gradient to be small enough in order to remain in the linear response regime. The temperature gradient along the Hall bar is a function of the dissipated power $P=R_hI_h^2$, in the region underneath gate $g1$. ΔT will thus be a function of the second harmonic of the heating current. The continuous gate $g1$ was used to partly deplete the 2DEG under the gate by applying a negative voltage to $g1$ relative to one of the 2DEG current contacts. This served two purposes. Firstly, it increased the dissipated power; secondly, the dissipation could be confined to a narrow region of the Hall bar underneath the gate. The gate voltage and the heating-current levels were carefully adjusted so that the two-terminal resistance $b1$-$b2$ was dominated by the gated region and yet remained independent of the heating-current level. $V_{g1}=-0.1$ V was found to increase the two-terminal resistance $b1$-$b2$ by approximately a factor of 10. This allowed heating currents up to 1.5 μA. The heating resistance increased with magnetic field as shown in the upper panel of Fig. 1, and the data had to be corrected for this increase. For magnetic fields above approximately 0.4 T, our phase-sensitive detection of the second harmonic broke down, and the phase of the signal started to depend on magnetic field. We have thus limited our analysis to fields below 0.4 T. Hence the absence of the $n=1$ peak. A first-harmonic signal was also generated, as a consequence of the nonlocal spreading resistance. This first-harmonic signal was roughly a factor of 2–3 (depending on heating current level) larger

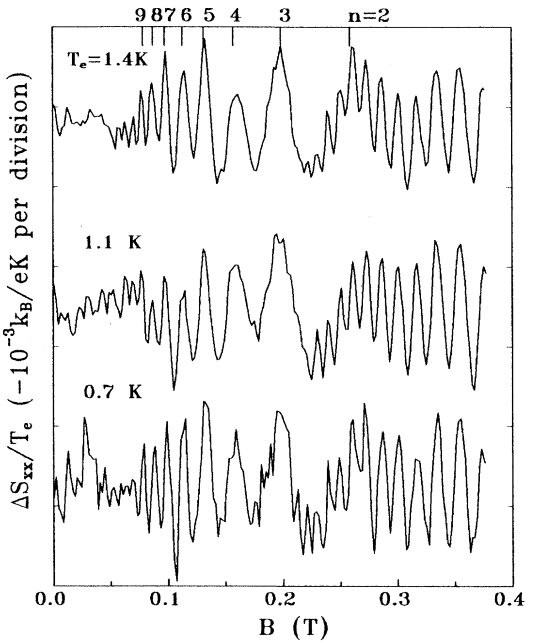

FIG. 4. The measured magnetothermopower divided by electron temperature for three values of electron temperatures. The curves have been offset for clarity. The zero-field levels for the three curves are -6.2, -7.5, and $-6.7\times10^{-3}k_BT_e/e$, respectively, from top to bottom. The similarity between the curves indicates that the measured thermopowers are proportional to the temperature. One can vaguely see an earlier onset of SdH oscillations as temperature is decreased. The commensurability oscillations are clearly seen and marked with their respective index numbers on the top of the figure. The data have been corrected for a magnetic-field dependence of the heating resistance as seen in Fig. 1.

than the second-harmonic signal at $B=0$ and exhibited a large positive magnetoresistance. The second-harmonic voltage response V_{2f} shown in Fig. 1 was obtained with a heating current of 1.2 μA. It should be noticed that the commensurability oscillations in V_{2f} are 90° out of phase with the oscillations in R_{xx}, whereas the SdH oscillations are roughly 180° out of phase. Theoretically it has been predicted[13] that the commensurability oscillations in the thermopower should be 90° out of phase with the oscillations in ρ_{xx}, i.e., in agreement with our experiment, while the SdH oscillations should be in phase for the two signals. We thus have a discrepancy with the theory regarding the SdH oscillations. The relative phase of the two measurements is, however, very sensitive to the determination of the zero of the magnetic field, which is subject to a small correction due to hysteresis in the superconducting solenoid. Moreover, we had to scale the magnetic-field axis for the two curves in the lower panel of Fig. 1 due to small differences in carrier density of the sample that occurred between the two measurements. We have thus very carefully corrected the data for the above-mentioned effects. It is also worthwhile to emphasize that no effect caused by a nonlinearity of the heating resistance could cause the observed phase relation between the commensurability oscillations and the SdH oscillations. We thus leave this discrepancy unexplained. We also note that the heating resistance is smooth and monotonic in the magnetic-field regime depicted. The SdH oscillations in the second-harmonic signal are thus not caused by SdH oscillations induced in the temperature gradient by oscillations in the dissipated power.

In order to extract the thermopower from the measured second-harmonic voltage we now determine the temperature difference between probes $c1$ and $d1$ induced by a heating current passed between contacts $b1$ and $b2$. This temperature difference could not be measured directly, basically because of the difficulties associated with measuring any temperature dependent quantity between each of the probe pairs $c1,c2$ and $d1,d2$ independently and without imposing additional grounds to the current circuit $b1,b2$. However, the electron temperature in the "hot" region between the current contacts $b1$ and $b2$ could be measured. This was done by exploiting the temperature dependence of the SdH oscillations in the two-terminal heating resistance $R_h(B)$ at magnetic fields higher than shown in Fig. 1. The important property for the temperature gradient is the dissipated power, which could be controlled either by the heating current or the heating resistance. The SdH oscillations in the heating resistance used to determine the electron temperature occurred at magnetic fields above 0.5 T, i.e., above the range where the thermopower measurements were done. However, we used lower current levels in the electron-temperature determination to keep the dissipated power comparable with the thermopower measurements. First, we recorded the SdH oscillations with a sufficiently low heating current for the electron temperature to approach the lattice temperature. This was done for various lattice temperatures. This set of measurements served as a reference for subsequent measurements with higher heating currents. An example of the reference-peak-height dependence on lattice (bath) temperature is shown in the inset (a) of Fig. 2. By comparing the peak heights for the high current data [inset (b) of Fig. 2] with the reference-peak heights, we were able to estimate the electron temperature $T_e=T_h$ in the hot region under the heating gate. This determination is shown in Fig. 2. It should be noticed that several SdH peaks could be used for this temperature calibration, each corresponding to a different heating resistance, and hence to different heating powers in the plot. The dissipated power must equal the heat loss to phonons, which empirically has been found to obey a characteristic power-law dependence on electron temperature:

$$P=R_hI_h^2=\alpha(T_e^{\gamma}-T_L^{\gamma}). \tag{2}$$

Experimentally $\gamma=3$ has been reported repeatedly.[16] We find a reasonable although not perfect fit to our data with $\gamma=3$. This fit is shown as the solid line in Fig. 2. Theoretically it has, however, been found that $\gamma=3$ has no fundamental significance, but rather marks a transition between a $\gamma=5$ dependence at low temperatures and a $\gamma=2$ dependence at high temperatures.[16] We thus use a power-function fit ($T_e\propto P^b$) with $b\approx0.5$ to represent the electron-temperature dependence on dissipated power. In order to estimate the electron-temperature difference between the voltage probes, we have solved the one-dimensional heat equation to find the electron temperature as a function of the distance x from the hot region under the heating gate. This was done assuming a phonon loss rate given by Eq. (2),

and asserting the boundary conditions $T_e(x=0)=T_h$, $T_e(x=\infty)=T_L$, and $dT_e/dx|_{x=\infty}=0$. Furthermore, we assumed that the power $P=R_hI_h^2$ was dissipated within an area of $A=20\times20$ μm^2. The differential equation for the heat conduction then reads as follows:

$$\frac{d}{dx}\left(K\frac{dT_e}{dx}\right)=\frac{\alpha}{A}(T_e^\gamma-T_L^\gamma), \tag{3}$$

where the heat conductivity K is given by Wiedemann-Franz law: $K=L\sigma_0T_e$ with the Lorentz number $L=\pi^2k_B^2/3e^2=2.45\times10^{-8}$ W Ω/K^2. After one integration, Eq. (3) can be rewritten to integral form as

$$x_{T_e}=-\eta\int_{T_h/T_L}^{T_e/T_L}(2\theta^\gamma-2-\gamma+\gamma\theta^{-2})^{-1/2}d\theta, \tag{4}$$

where x_{T_e} is the position where the temperature is T_e. Equation (4) can easily be integrated numerically with

$$\eta=\left(\frac{\gamma+2}{\alpha\sigma_0/LA}\right)^{1/2}T_L^{(2+\gamma)/2}\approx100\ \ \mu\text{m}$$

for $\gamma=3$, $T_L=0.35$ K, and $\sigma_0\approx(11\ \Omega)^{-1}$, applicable to the experimental conditions. In Fig. 3 we show plots of (T_e,x) for various boundary values T_h/T_L at $x=0$. The temperature difference between the positions adjacent to the voltage probes and the average electron temperature between the probes can then simply be evaluated from the plot in Fig. 3 [or from Eq. (4) directly]. This gives temperature differences of the order 0.25 K, and $\Delta T/T_L\approx0.2$. This analysis is off course based on too many assumptions to give 100% reliable values for the temperature difference. However, we believe that the values we get are within 50% from the real values and do not change the conclusions qualitatively. In Fig. 4 we have plotted the resulting thermopowers as $[S_{xx}(B)-S_{xx}(0)]/T_e$, with $S_{xx}(0)=-(7\times10^{-3}\pm2\times10^{-3})k_BT_e/e$. This zero-field value compares favorably with what is expected for the diffusion thermopower for a degenerate electron gas,[12] namely, $S\approx-(k_B/e)(k_BT_e/\varepsilon_F)$, which for our Fermi energies gives $S=-7.9\times10^{-3}k_BT_e/e$. It is also obvious from our data that the thermopower has linear dependence on electron temperature as expected from theory. The amplitude of our oscillations is about a factor of 5 smaller than calculated in Ref. 13; however, their thermopower oscillations are calculated for a modulation amplitude of $V_0=0.5$ mV. The modulation amplitude can be determined from the position of the maximum of the positive magnetoresistance in $\rho_{xx}(B)$. The positive magnetoresistance below 0.02 T is caused by electrons that are forced to move in open (streaming) orbits along the stripes because the magnetic Lorentz force $e\mathbf{v}_F\times\mathbf{B}$ exerted on them is unable to lift them over the potential barriers imposed by the modulation.[17] The maximum in the modulation thus occurs at a critical magnetic field given by $ev_FB_c=2\pi eV_0/a$. Inserting $B_c=0.018$ T we get $V_0=0.26$ mV. If we assume that the amplitude of the thermopower oscillations depends on V_0^2, our data ought to be a factor of about 4 smaller than in Ref. 13, which is in remarkably good agreement with the reference.

In conclusion, we have measured the diffusion thermopower in the linear response regime for a lateral superlattice, and found commensurability oscillations. Our data are in good agreement with theory with respect to both the temperature dependence and the size of the effect. Concerning the phase relation between the observed oscillations in the magnetothermopower and the magnetoresistance we find an unexplained (180°) disagreement with the theory regarding the SdH oscillations in Ref. 13. The existing quantum-mechanical theory, however, appears rather complex, and one could hope that a more physically appealing semiclassical theory could be developed for the thermal properties of later superlattices. In fact, a semiclassical theory for the oscillations in ρ_{yy} based on small-angle scattering has very recently been developed.[18]

One of the authors (R.T.) is grateful for a "Human Capital and Mobility" research fellowship from the EU that made this work possible. We thank Dr. M. Field and Dr. G. A. C. Jones for technical support. We would also like to acknowledge many helpful discussions with Dr. A. S. Dzurak, Dr. C. G. Smith, Dr. A. R. Hamilton, Dr. C. Barnes, Dr. P. E. Lindelof, and Dr. D. H. Cobden. We thank Dr. A. Smith and Dr. P. Hedegaard for presenting their theory to us prior to publication.

*Present address: Physics Dept., Technical University of Denmark, Bldg. 309, DK-2800 Lyngby, Denmark.

[1] D. Weiss *et al.*, Europhys. Lett. **8**, 179 (1989).
[2] R. W. Winkler *et al.*, Phys. Rev. Lett. **62**, 1177 (1989).
[3] C. G. Smith *et al.*, J. Phys. C **2**, 3405 (1990).
[4] R. R. Gerhardts *et al.*, Phys. Rev. Lett. **62**, 1173 (1989).
[5] C. W. J. Beenakker, Phys. Rev. Lett. **62**, 2020 (1989).
[6] P. Vasilopoulos and F. M. Peeters, Phys. Rev. Lett. **63**, 2120 (1989).
[7] C. Zhang and R. R. Gerhardts, Phys. Rev. B **41**, 12 850 (1990).
[8] D. Phannkuche and R. R. Gerhardts, Phys. Rev. B **46**, 12 606 (1992).
[9] P. Boggild *et al.*, Phys. Rev. B **51**, 7336 (1995).
[10] J. H. Davies and I. A. Larkin, Phys. Rev. B **49**, 4800 (1994).
[11] G. Muller *et al.*, Phys. Rev. B **50**, 8938 (1994).
[12] B. L. Gallagher and P. N. Butcher, in *Handbook on Semiconductors*, edited by T. S. Moss (Elsevier, Amsterdam, 1992), pp. 721–816.
[13] F. M. Peeters and P. Vasilopoulos, Phys. Rev. B **46**, 4667 (1992); **42**, 5899 (1990).
[14] P. W. Anderson *et al.*, Phys. Rev. Lett. **43**, 718 (1979).
[15] See, for example, M. C. Payne *et al.*, J. Phys. C **16**, L291 (1983); R. T. Syme *et al.*, *ibid.* **1**, 3375 (1989); L. Gallagher *et al.*, Phys. Rev. Lett. **64**, 2058 (1990); L. W. Molenkamp *et al.*, *ibid.* **65**, 1052 (1990); A. S. Dzurak *et al.*, Solid State Commun. **87**, 1145 (1993).
[16] Y. Ma *et al.*, Phys. Rev. B **43**, 9033 (1991), and references therein.
[17] P. H. Beton *et al.*, Phys. Rev. B **42**, 9229 (1990).
[18] A. Smith and P. Hedegaard (unpublished).